



Linking hierarchical stratal architecture to plume spreading in a Lagrangian-based transport model

Ramya Ramanathan,¹ Robert W. Ritzi Jr.,¹ and Chaocheng Huang²

Received 18 June 2007; revised 10 November 2007; accepted 16 January 2008; published 17 April 2008.

[1] In this article we present a new formulation of the Lagrangian-based model for macrodispersion of inert solutes. The formulation is based on a hierarchical expression of the spatial covariance of log permeability developed from recent findings at the well-studied Borden research site. The covariance expression represents a two-level hierarchy of stratal unit types with a corresponding hierarchy of permeability subpopulations. The covariance is a linear sum of terms corresponding to the probability of transitioning across stratal unit types of different scales, and these terms are directly related to quantifiable geometric attributes of the hierarchical stratal architecture at the Borden site. The new macrodispersion model is also a linear sum of terms, with different integral scales defined by the hierarchy of cross-transition probabilities and computed from the proportions and length statistics of the stratal unit types. The model allows the study of the contribution of each term to the composite particle displacement variance and thus the study of how the hierarchical stratal architecture influences plume spreading.

Citation: Ramanathan, R., R. W. Ritzi Jr., and C. Huang (2008), Linking hierarchical stratal architecture to plume spreading in a Lagrangian-based transport model, *Water Resour. Res.*, 44, W04503, doi:10.1029/2007WR006282.

1. Introduction

[2] The Lagrangian development of a model for macrodispersion was initially based on representing the spatial covariance of log conductivity, $\ln(K)$, with a single, finite, integral scale [e.g., Dagan, 1982, 1984]. The model explained, quite well, the particle displacement variance observed in the well-known Borden natural gradient tracer test [Sudicky, 1986; Woodbury and Sudicky, 1991]. Newer work at the Borden site has shown that the Borden aquifer sediment comprises a hierarchy of sedimentary unit types and that the $\ln(K)$ covariance comprises a corresponding hierarchy of integral scales [Ritzi and Allen-King, 2007]. This article derives and discusses the corresponding Lagrangian-based macrodispersion model.

[3] We build on the foundation of work which has advanced both the models for the spatial bivariate statistics of log permeability (correlation models hereafter), and the corresponding models for macrodispersion [see Rubin, 1995; Barrash and Clemo, 2002; Lu and Zhang, 2002; Neuman, 2003; Ritzi et al., 2004; Dai et al., 2005; Neuman, 2006; Ritzi et al., 2006; Rubin et al., 2006; Ritzi and Allen-King, 2007]. Our focus is on work that has made a stronger link with geology. Such linkage has been achieved by combining the geostatistics of integer indicator variables representing the sedimentary architecture, with the geostatistics of continuous variables representing $\ln(K)$ within each sedimentary unit type. Developing correlation models with this approach creates direct mathematical linkages

between the structure(s) of the correlation model, and quantifiable physical attributes of the sedimentary architecture including the proportion of unit types, their mean and variance in length, and the resulting probabilities for cross transitions at each hierarchical level. In some cases, it was shown that the shape and range of the composite permeability correlation structure(s) can be determined from just those attributes of the hierarchical sedimentary architecture, and that only univariate $\ln(K)$ statistics were needed to scale ordinate [Ritzi et al., 2004; Dai et al., 2005; Ritzi and Allen-King, 2007].

[4] A number of practical benefits are derived from this approach. Mathematically linking the shape and range of the correlation model to quantifiable physical attributes of the sedimentary architecture provides a rational basis for choosing a particular correlation structure and for computing the associated integral scale(s). Thus, it helps avoid the often equivocal fitting of curves to sample bivariate statistics inherent in traditional approaches (see discussion by Ritzi and Allen-King [2007]). Furthermore, lithologic data and related information about the sedimentary architecture which are used are often easier to obtain and therefore more abundant than $\ln(K)$ data [e.g., Weissmann and Fogg, 1999; Weissmann et al., 1999; Proce et al., 2004; Dai et al., 2005; Rubin et al., 2006]. Dai et al. [2005] have shown that developing correlation models with this approach provides a better understanding of how bias arises from data locations, and leads to ways of avoiding or reducing such bias.

[5] Prior work [e.g., Rubin, 1995; Dai et al., 2004; Rubin et al., 2006] has incorporated these hierarchical, geologically based correlation models into derivations of macrodispersion models. These macrodispersion models are subsets of the more general model derived below. All of the practical benefits associated with the hierarchical, geologically based correlation models, discussed above, trans-

¹Department of Earth and Environmental Sciences, Wright State University, Dayton, Ohio, USA.

²Department of Mathematics and Statistics, Wright State University, Dayton, Ohio, USA.

fer directly to the models for macrodispersion. Furthermore, these macrodispersion models link the process of mechanical dispersion to quantifiable physical attributes of sedimentary unit types at each scale. The distance to reach the large time limit of macrodispersivity can also be directly linked to the existence of these unit types. Thus, the approach leads to a model which potentially is easier and less expensive to develop and provides new and additional insights.

[6] This article is a logical extension of *Ritzi and Allen-King* [2007]. Here we derive the Lagrangian-based macrodispersion model that corresponds to the correlation model which they developed with these hierarchical, geologically based methods using the new data from the Borden site. We first review and summarize their correlation model, and then show that its nature requires us to extend the results of *Dai et al.* [2004] and *Rubin et al.* [2006] in developing the appropriate Lagrangian-based expressions for the particle displacement variance and macrodispersivity. At the rigorously studied Borden site, this approach leads to calculating essentially the same statistical moments for the solute plume as in prior studies [cf. *Sudicky*, 1986; *Woodbury and Sudicky*, 1991], however, we are able to better link dispersion to quantifiable physical attributes of the sedimentary architecture, which previously has been a matter of speculation. As argued above, the benefits of applying this approach at sites where $\ln(K)$ data are less abundant than at Borden, may be even more significant.

2. Review of the Hierarchical, Geologically Based Correlation Model

[7] *Ritzi and Allen-King* [2007] delineated the sediments occurring in the experimental zone at Borden, on the basis of textural attributes, into a two-level hierarchy of unit types, as illustrated in Figure 1. To briefly explain how the spatial bivariate statistics for log permeability are linked to this architecture, we first define some symbols. Consider locations \mathbf{x} and \mathbf{x}' which are separated by a lag vector \mathbf{h} . Consider that location \mathbf{x} is within level I (smaller-scale) unit type o which, in turn, is within level II (larger-scale) unit type r (the location will be referred to as in region type ro hereafter), and that \mathbf{x}' is within level I unit type i which is within level II unit type j (region type ji). Using this hierarchy of subscripts, the composite sample semivariogram was written, following *Ritzi et al.* [2004], with designation of regions types into which the heads and tails of \mathbf{h} fall:

$$\begin{aligned} \hat{\gamma}(\mathbf{h}) = & \sum_r \sum_o \hat{\gamma}_{ro,ro}(\mathbf{h}) \hat{p}_{ro}(\mathbf{h}) \hat{t}_{ro,ro}(\mathbf{h}) \\ & + \sum_r \sum_o \sum_{i \neq o} \hat{\gamma}_{ro,ri}(\mathbf{h}) \hat{p}_{ro}(\mathbf{h}) \hat{t}_{ro,ri}(\mathbf{h}) \\ & + \sum_r \sum_{j \neq r} \sum_o \sum_{i \neq o} \hat{\gamma}_{ro,ji}(\mathbf{h}) \hat{p}_{ro}(\mathbf{h}) \hat{t}_{ro,ji}(\mathbf{h}) \end{aligned} \quad (1)$$

Here the $\hat{\gamma}_{ro,ji}(\mathbf{h})$ are the autosemivariograms and cross-semivariograms [$ro = ji$ and $ro \neq ji$, respectively] as defined by head and tail region type. The $\hat{t}_{ro,ji}(\mathbf{h})$ are the transition probabilities which give the fraction of lags of a particular distance and direction that transition to region type ji given they start in region type ro . The proportions $\hat{p}_{ro}(\mathbf{h})$ give the fraction of lags that start in region type ro . The first of the three groups of terms on the RHS of equation (1) is referred to as the $\alpha\alpha$ autotransition group, corresponding to lags that are

autotransitions at both levels II and I. The second group is the $\alpha\chi$ cross-transition group (autotransitions at level II, cross transitions at level I). The third group is the $\chi\chi$ cross-transition group (cross transitions at both levels II and I).

[8] *Ritzi and Allen-King* [2007] used two sets of colocated data, one with permeability as a continuous variable, and the other with stratal designation based on an integer indicator variable, to evaluate the relative contribution of the terms in equation (1). In both vertical and horizontal directions, the shape and the range of the composite semivariogram were determined by the $\hat{p}_{ro}(\mathbf{h}) \hat{t}_{ro,ji}(\mathbf{h})$ for $r \neq j$ and/or $o \neq i$ terms. In other words, the shape and range were determined by how the probability of $\alpha\chi$ and $\chi\chi$ cross transitions grew with lag distance. The $\hat{\gamma}_{ro,ji}(\mathbf{h})$ were well approximated by constants, and essentially weight the contributions of the $\hat{p}_{ro}(\mathbf{h}) \hat{t}_{ro,ji}(\mathbf{h})$ the same regardless of lag distance. The $\alpha\alpha$ group was insignificant and could be ignored. Thus, the semivariogram structure was found to be determined by the stratal architecture, independent of permeability values. These findings were similar to those in analyses of data representing other deposits by *Ritzi et al.* [2004] and *Dai et al.* [2005].

[9] In all of these three prior studies a parsimonious semivariogram model could be developed, without curve fitting, from univariate statistics for the proportion and length of unit types, and univariate statistics for permeability as divided into subpopulations by unit type, for each level. In this approach, the hierarchical levels are considered individually. First, at each level, the coefficient of variation for the lengths of the unit types are evaluated, and a transition probability model is chosen on the basis of its value, following relationships defined by *Ritzi* [2000]. *Ritzi and Allen-King* [2007] found that the coefficient of variation for lengths of unit types at each level were of the order of unity and, following *Ritzi* [2000], chose exponential functions to represent the $\hat{p}_{ro}(\mathbf{h}) \hat{t}_{ro,ji}(\mathbf{h})$ for $\alpha\chi$ and $\chi\chi$ cross transitions. Second, the $\hat{\gamma}_{ro,ji}(\mathbf{h})$ are approximated by constant weights:

$$\begin{aligned} \gamma(h) = & \sum_r \sum_o \sum_{i \neq o} \frac{1}{2} \left[\sigma_{ro}^2 + \sigma_{ri}^2 + (m_{ro} - m_{ri})^2 \right] p_{ro} p_{ri} \left(1 - e^{-\frac{h}{\lambda_{\alpha\chi}}} \right) \\ & + \sum_r \sum_{j \neq r} \sum_o \sum_{i \neq o} \frac{1}{2} \left[\sigma_{ro}^2 + \sigma_{ji}^2 + (m_{ro} - m_{ji})^2 \right] \\ & \cdot p_{ro} p_{ji} \left(1 - e^{-\frac{h}{\lambda_{\chi\chi}}} \right) \end{aligned} \quad (2)$$

and thus the mean and variance for permeability subpopulations (m_{ro} , σ_{ro}^2) represent permeability variation in the heads and tails of cross transitions, and define the ordinate scaling of the semivariogram. (Here the model is written for a specific direction of interest in which unit lengths are characterized, and h is the magnitude of \mathbf{h} in that direction.) Third, the indicator integral scale for the $\alpha\chi$ cross-transition term (across smaller-scale level I unit types) is given by $\lambda_{\alpha\chi} = \bar{l}_o(1 - p_o)$, where \bar{l}_o is the mean length of unit type o , and for the $\chi\chi$ cross-transition term (across larger-scale level II unit types) by $\lambda_{\chi\chi} = \bar{l}_r(1 - p_r)$. Semivariogram models in the form of equation (2), with parameters determined this way, have represented the sample semivariogram quite well in these studies [*Ritzi et al.*, 2004; *Dai et al.*, 2005; *Ritzi and Allen-King*, 2007].

[10] Evaluating the spatial bivariate statistics for permeability with equations (1) and (2) gives insight into how the composite semivariogram comprises two correlation structures, each with different integral scales that correspond to

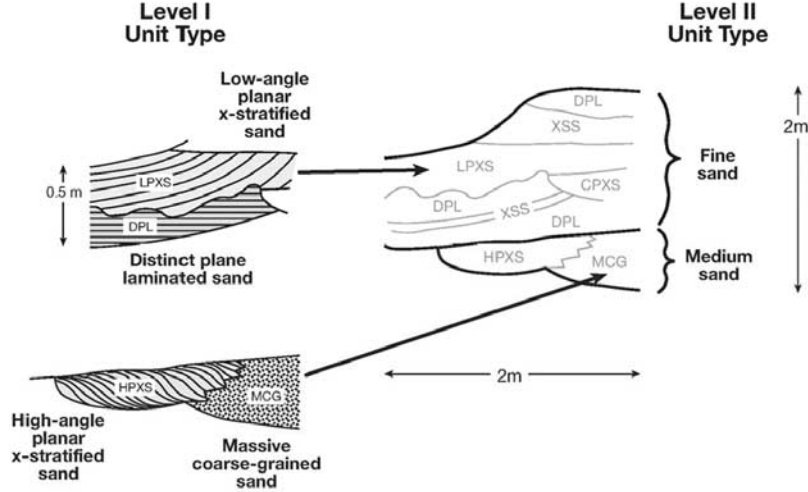


Figure 1. Sedimentary architecture exposed on an outcrop at the Borden site [from *Ritzi and Allen-King, 2007*].

two different scales of stratal unit types. The model in equation (2) directly links the composite semivariogram with the proportions and length statistics for these unit types, and thus links them to quantifiable physical attributes of the hierarchical stratal architecture. By deriving expressions for macrodispersion from equation (2), we can make a link between the composite particle displacement variance and quantifiable physical attributes of the hierarchical stratal architecture. The motivation is not so much to gain better predictions, but rather to gain better insight into how hierarchical stratal architecture affects plume spreading.

[11] In this vein, *Dai et al.* [2004] reviewed prior work in using hierarchical expressions for spatial bivariate statistics in deriving Lagrangian-based macrodispersion models. All prior models, including that of *Dai et al.* [2004], assume a single integral scale for the hierarchy of cross-transition probabilities. Thus, they do not represent the case in equation (2), where the cross-transition probabilities defined at level II have a larger integral scale $\lambda_{\chi\chi}$, as compared to that for cross-transition probabilities defined at level I, $\lambda_{\alpha\chi}$. The goal of this article is to derive a Lagrangian-based expression for macrodispersion from the hierarchical correlation structure represented in the form of equation (2), and explore the contribution of each term to the composite particle displacement variance.

3. Methodology

[12] Writing equation (2) in the form of the centered covariance gives [see *Ritzi et al., 2004*, appendix]

$$C_Y(h) = \sigma_Y^2 - \sum_r \sum_o \sum_{i \neq o} \frac{1}{2} \left[\sigma_{ro}^2 + \sigma_{ri}^2 + (m_{ro} - m_{ri})^2 \right] \cdot p_{ro} p_{ri} \left(1 - e^{-\frac{h}{\lambda_{\alpha\chi}}} \right) - \sum_r \sum_{j \neq r} \sum_o \sum_{i \neq o} \frac{1}{2} \left[\sigma_{ro}^2 + \sigma_{ji}^2 + (m_{ro} - m_{ji})^2 \right] \cdot p_{ro} p_{ji} \left(1 - e^{-\frac{h}{\lambda_{\chi\chi}}} \right) \quad (3)$$

[13] Rearranging the terms on RHS and regrouping:

$$C_Y(h) = \sigma_Y^2 - \sum_r \sum_o \sum_{i \neq o} \frac{1}{2} \left[\sigma_{ro}^2 + \sigma_{ri}^2 + (m_{ro} - m_{ri})^2 \right] p_{ro} p_{ri} - \sum_r \sum_{j \neq r} \sum_o \sum_{i \neq o} \frac{1}{2} \left[\sigma_{ro}^2 + \sigma_{ji}^2 + (m_{ro} - m_{ji})^2 \right] p_{ro} p_{ji} + \sum_r \sum_o \sum_{i \neq o} \frac{1}{2} \left[\sigma_{ro}^2 + \sigma_{ri}^2 + (m_{ro} - m_{ri})^2 \right] p_{ro} p_{ri} e^{-\frac{h}{\lambda_{\alpha\chi}}} + \sum_r \sum_{j \neq r} \sum_o \sum_{i \neq o} \frac{1}{2} \left[\sigma_{ro}^2 + \sigma_{ji}^2 + (m_{ro} - m_{ji})^2 \right] p_{ro} p_{ji} e^{-\frac{h}{\lambda_{\chi\chi}}} \quad (4)$$

[14] It can be shown that the sum of the first three terms, referred to as R hereafter, has a small and constant value, and can be ignored to help make the derivation tractable. This follows from the fact that the composite variance, σ_Y^2 , can be written as [*Ritzi et al., 2004*]

$$\sigma_Y^2 = \sum_r \sum_o p_{ro} \sigma_{ro}^2 + \frac{1}{2} \sum_r \sum_o \sum_{i \neq o} p_{ro} p_{ri} [m_{ro} - m_{ri}]^2 + \frac{1}{2} \sum_r \sum_{j \neq r} \sum_o \sum_{i \neq o} p_{ro} p_{ji} [m_{ro} - m_{ji}]^2$$

and that

$$\sum_r \sum_o p_{ro} = 1$$

so that

$$R = \sum_r \sum_o p_{ro} \sigma_{ro}^2 p_{ro} p_{ri} + \frac{1}{2} \sum_r \sum_o \sum_{i \neq o} p_{ro} p_{ri} [m_{ro} - m_{ri}]^2 + \frac{1}{2} \sum_r \sum_{j \neq r} \sum_o \sum_{i \neq o} p_{ro} p_{ji} [m_{ro} - m_{ji}]^2 - \sum_r \sum_o \frac{1}{2} \left[\sigma_{ro}^2 \right] p_{ro} \sum_{j \neq r} \sum_{i \neq o} p_{ji} - \sum_{j \neq r} \sum_{i \neq o} \frac{1}{2} \left[p_{ji} \sigma_{ji}^2 \right] - \sum_r \sum_o \sum_{i \neq o} \frac{1}{2} [m_{ro} - m_{ri}]^2 p_{ro} p_{ri} - \sum_r \sum_{j \neq r} \sum_o \sum_{i \neq o} \frac{1}{2} [m_{ro} - m_{ji}]^2 p_{ro} p_{ji}$$

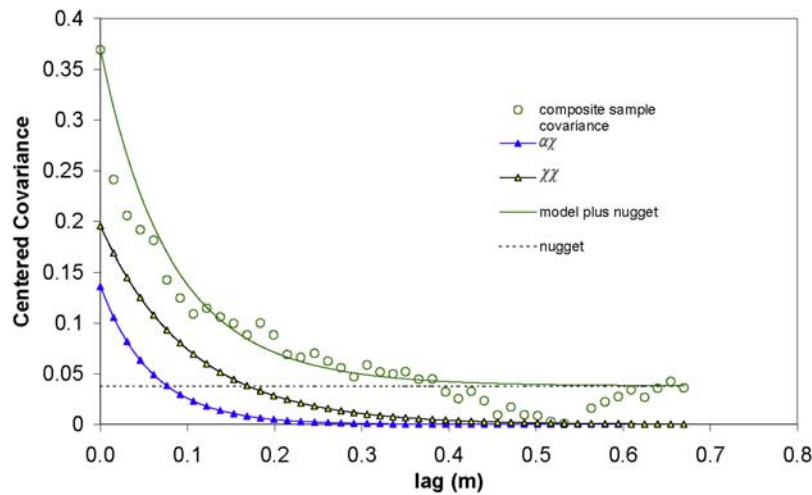


Figure 2. Centered covariance model compared to the vertical sample covariance. Note the model curve is not fitted but is developed from univariate statistics for length and permeability. Also shown are the relative contributions from the $\alpha\chi$ and the $\chi\chi$ terms.

which simplifies to

$$R = \sum_r \sum_o \sigma_{ro}^2 p_{ro}^2 \quad (6)$$

[15] With the data *Ritzi and Allen-King* [2007] used, σ_Y^2 equals 0.369 and R equals 0.038. Thus R is a relatively small nugget in the centered covariance model, and nugget does not affect dispersion [Rubin, 2003]. Neglecting R (for now), equation (3) takes the form

$$C_Y(h) = \sum_r \sum_o \sum_{i \neq o} \frac{1}{2} [\sigma_{ro}^2 + \sigma_{ri}^2 + (m_{ro} - m_{ri})^2] p_{ro} p_{ri} e^{-\frac{h}{\lambda_{\alpha\chi}}} + \sum_r \sum_{j \neq r} \sum_o \sum_{i \neq o} \frac{1}{2} [\sigma_{ro}^2 + \sigma_{ji}^2 + (m_{ro} - m_{ji})^2] p_{ro} p_{ji} e^{-\frac{h}{\lambda_{\chi\chi}}} \quad (7)$$

which can be written as

$$C_Y(h) = A e^{-\frac{h}{\lambda_{\alpha\chi}}} + B e^{-\frac{h}{\lambda_{\chi\chi}}} \quad (8)$$

where

$$A = \sum_r \sum_o \sum_{i \neq o} \frac{1}{2} [\sigma_{ro}^2 + \sigma_{ri}^2 + (m_{ro} - m_{ri})^2] p_{ro} p_{ri} \quad \text{and} \\ B = \sum_r \sum_{j \neq r} \sum_o \sum_{i \neq o} \frac{1}{2} [\sigma_{ro}^2 + \sigma_{ji}^2 + (m_{ro} - m_{ji})^2] p_{ro} p_{ji}$$

The composite integral scale is given by

$$\lambda = \frac{1}{\sigma_Y^2} \int_0^\infty C_Y(h) dh = \frac{1}{\sigma_Y^2} [A \lambda_{\alpha\chi} + B \lambda_{\chi\chi}] \quad (9)$$

Thus, the composite integral scale computed by *Sudicky* [1986] lumps together the $\alpha\chi$ and the $\chi\chi$ scales of permeability correlation, as respectively weighted by A/σ_Y^2 and B/σ_Y^2 . Furthermore, if both the $A\lambda_{\alpha\chi}$ and $B\lambda_{\chi\chi}$ terms contribute significantly in (9), then the composite integral

scale, λ , will not be well characterized unless both $A\lambda_{\alpha\chi}$ and $B\lambda_{\chi\chi}$ are well characterized. This implies that the mean and variance in length of both level I and level II unit types must be well characterized in the direction the spatial covariance is computed (see extensive discussion in context of the Borden site by *Ritzi and Allen-King* [2007]).

[16] Figure 2 shows the vertical composite sample covariance computed using the permeability data from *Ritzi and Allen-King* [2007]. The covariance model (8) is also plotted, as defined by the statistics of *Ritzi and Allen-King* [2007]. These statistics include the mean and variance for the permeability subpopulations, the proportions of the unit types, and the $\alpha\chi$ and $\chi\chi$ integral scales computed from thickness statistics. (Note they reported effective ranges, a , where $[a_{\alpha\chi} = 3\lambda_{\alpha\chi} = 0.18 \text{ m}; a_{\chi\chi} = 3\lambda_{\chi\chi} = 0.31 \text{ m}]$. The contributions of each of the $\alpha\chi$ and $\chi\chi$ terms in equation (8) are also plotted. The longer correlation structure of the $\chi\chi$ term is evident, as is the fact that it contributes relatively more to the composite covariance. Indeed, *Ritzi and Allen-King* [2007] showed that there are a larger proportion of $\alpha\chi$ cross transitions at any given lag, however, the differences in permeability across level II unit types in the heads and tails of $\chi\chi$ lags are larger so the $\chi\chi$ term contributes more to the model. The model in equation (8) is a good representation of the vertical composite covariance. There is a small difference at lag zero between the sample and the model covariances, because of neglecting $\sum_r \sum_o \sigma_{ro}^2 p_{ro}^2$, which could be added back in as a nugget structure if desired.

4. Derivation of Macrodispersivity Tensor and Particle Displacement Variance

[17] The macrodispersivity tensor is derived by *Dagan* [1989], *Rubin* [1995], and *Dai et al.* [2004] from the velocity covariance, \widehat{u}_{ij} :

$$\widehat{u}_{ij}(k) = U_1^2 \left[\delta_{1i} - \frac{k_1 k_i}{k^2} \right] \left[\delta_{1j} - \frac{k_1 k_j}{k^2} \right] \widehat{C}_Y(k) \quad (i, j = 1, 2, \dots, d) \quad (10)$$

where the circumflex denotes the Fourier transform operator, $U_1 = \frac{G e^{\beta \gamma}}{n_{eff}}$ is the mean velocity, G is the average hydraulic gradient, and n_{eff} is the effective porosity. The average gradient is assumed to be aligned with the principal axis. The other assumptions under which equation (10) is derived (following *Rubin* [2003] and *Dai et al.* [2004]) include (1) steady state flow, (2) uniform velocity field, (3) unbounded flow domain, (4) weak stationarity of log conductivity, (5) and the variance of log conductivity is less than unity. Using equation (10) and assuming that the solute velocity is approximated at first order, the macrodispersion tensor is computed by

$$D_{ij}(t) = \int_0^t u_{ij}(U_1 t') dt' \quad (11)$$

[18] Combining the Fourier transform of (8) with (10)–(11), the 2-D macrodispersivity coefficients are

$$\begin{aligned} \frac{D_{11}(t)}{U_1} = & \beta A \lambda_{\alpha\chi} \left[1 + \frac{3}{2 \exp(\tau_{\alpha\chi}) \tau_{\alpha\chi}^3} \left(2(\exp(\tau_{\alpha\chi}) - \tau_{\alpha\chi} - 1) \right. \right. \\ & \left. \left. - \exp(\tau_{\alpha\chi}) \tau_{\alpha\chi}^2 \right) \right] \\ & + \beta B \lambda_{\chi\chi} \left[1 + \frac{3}{2 \exp(\tau_{\chi\chi}) \tau_{\chi\chi}^3} \left(2(\exp(\tau_{\chi\chi}) - \tau_{\chi\chi} - 1) \right. \right. \\ & \left. \left. - \exp(\tau_{\chi\chi}) \tau_{\chi\chi}^2 \right) \right] \quad (12) \end{aligned}$$

$$\begin{aligned} \frac{D_{22}(t)}{U_1} = & \beta A \lambda_{\alpha\chi} \left[\frac{6[1 - \exp(\tau_{\alpha\chi}) + \tau_{\alpha\chi}] + 2\tau_{\alpha\chi}^2 + \exp(\tau_{\alpha\chi}) \tau_{\alpha\chi}^2}{2 \exp(\tau_{\alpha\chi}) \tau_{\alpha\chi}^3} \right] \\ & + \beta B \lambda_{\chi\chi} \left[\frac{6[1 - \exp(\tau_{\chi\chi}) + \tau_{\chi\chi}] + 2\tau_{\chi\chi}^2 + \exp(\tau_{\chi\chi}) \tau_{\chi\chi}^2}{2 \exp(\tau_{\chi\chi}) \tau_{\chi\chi}^3} \right] \quad (13) \end{aligned}$$

where $\tau_{\alpha\chi} = tU_1/\lambda_{\alpha\chi}$ and $\tau_{\chi\chi} = tU_1/\lambda_{\chi\chi}$ are the dimensionless time. To compare with *Sudicky's* [1986] 2-D model, we have also added his β which is an ad hoc parameter accounting for the vertical averaging of concentration data before computing the observed tracer moments. (Note that *Dagan* [1989] later introduced speculation about how β relates to stratification, but *Sudicky's* expressed motivation was simply to account for the reduction in variance from vertical averaging of the tracer data and had nothing to do with the stratification of the sediments. We introduce β into the 2-D model here so as to make a level comparison below to *Sudicky's* model and the vertically averaged tracer concentration data. We also give the 3-D version of these equations below, without the β factor.) In application, *Sudicky* [1986] computed β from the ratio of the variances of the vertically averaged and the three-dimensional permeability data which is 0.74.

[19] The large-time asymptotic limit of the longitudinal dispersion coefficient is

$$\frac{D_{\infty,11}(t)}{U_1} = \beta A \lambda_{\alpha\chi} + \beta B \lambda_{\chi\chi} \quad (14)$$

when the relative contributions from the $\alpha\chi$ and $\chi\chi$ terms are constant.

[20] To compare results to those of *Sudicky* [1986] requires the 2-D particle displacement variance. The particle displacement variance is related to the macrodispersivity coefficient by

$$X_{11}(t) = 2 \int_0^t \frac{D_{11}(t)}{U_1} dt; \quad X_{22}(t) = 2 \int_0^t \frac{D_{22}(t)}{U_1} dt \quad (15)$$

and the substitution of equations (12) and (13) into (15) gives expressions for the longitudinal and lateral particle displacement variance, $X_{11}(t)$ and $X_{22}(t)$:

$$\begin{aligned} X_{11} = & \beta A \lambda_{\alpha\chi}^2 \left\{ 2\tau_{\alpha\chi} - 3 \ln(\tau_{\alpha\chi}) + \frac{3}{2} - 3E + 3Ei(-\tau_{\alpha\chi}) \right. \\ & \left. + 3 \left[\frac{e^{-\tau_{\alpha\chi}} + e^{-\tau_{\alpha\chi}} \tau_{\alpha\chi} - 1}{(\tau_{\alpha\chi})^2} \right] \right\} \\ & + \beta B \lambda_{\chi\chi}^2 \left\{ 2\tau_{\chi\chi} - 3 \ln(\tau_{\chi\chi}) + \frac{3}{2} - 3E + 3Ei(-\tau_{\chi\chi}) \right. \\ & \left. + 3 \left[\frac{e^{-\tau_{\chi\chi}} + e^{-\tau_{\chi\chi}} \tau_{\chi\chi} - 1}{(\tau_{\chi\chi})^2} \right] \right\} \quad (16) \end{aligned}$$

$$\begin{aligned} X_{22} = & \beta A \lambda_{\alpha\chi}^2 \left\{ \frac{3}{\tau_{\alpha\chi}^2} + \ln(\tau_{\alpha\chi}) - \frac{3}{2} + E - Ei(-\tau_{\alpha\chi}) \right. \\ & \left. - 3 \left[\frac{e^{-\tau_{\alpha\chi}} [1 + \tau_{\alpha\chi}]}{\tau_{\alpha\chi}^2} \right] \right\} \\ & + \beta B \lambda_{\chi\chi}^2 \left\{ \frac{3}{\tau_{\chi\chi}^2} + \ln(\tau_{\chi\chi}) - \frac{3}{2} + E - Ei(-\tau_{\chi\chi}) \right. \\ & \left. - 3 \left[\frac{e^{-\tau_{\chi\chi}} [1 + \tau_{\chi\chi}]}{\tau_{\chi\chi}^2} \right] \right\} \quad (17) \end{aligned}$$

where E is the Euler constant and Ei is the exponential integral.

[21] We see that the first terms on the RHS of equations (16) and (17) give the contribution to plume spreading due to the $\alpha\chi$ cross-transition terms in the permeability covariance. The second terms give the contribution due to the $\chi\chi$ cross-transition terms. The model is used here to study the relative contributions of each of these terms, individually, to the composite particle displacement variance. Also, normalized sensitivity coefficients, $\left[\frac{\partial f(\alpha, t)}{\partial \alpha} \right]_{m_\alpha}$, where m_α is the local value of the parameter α , are

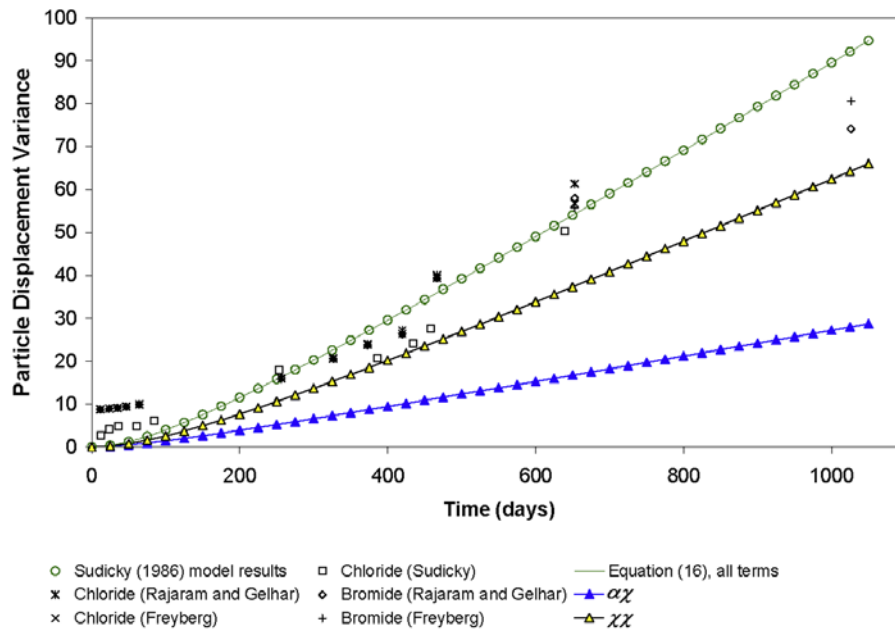


Figure 3. Plot of the longitudinal particle displacement variance, as compared to the *Sudicky* [1986] model and the observed tracer moments [See *Rajaram and Gelhar*, 1991; *Freyberg*, 1986].

computed (Appendix A) to study how model parameter sensitivity evolves with time [*Benjamin and Cornell*, 1970].

[22] We can illustrate using the model by considering the Borden site, but must first make clear some limitations of current data. *Ritzi and Allen-King* [2007] show that the current data are useful in identifying that the vertical or horizontal spatial bivariate structure for permeability is determined by the $\hat{p}_{ro}(\underline{h})\hat{t}_{ro,ji}(\underline{h})$ cross terms. The near exhaustive vertical sampling allows defining the vertical $[\lambda_{\alpha\chi}, \lambda_{\chi\chi}]$, as shown above. However, the 1 m spacing of the cores is not fine enough to capture the horizontal $\lambda_{\alpha\chi}$, and the 10 m transect of cores is not long enough to capture the horizontal $\lambda_{\chi\chi}$. The variance and mean of horizontal lengths of level I and level II unit types are severely

underestimated because of these limitations in data locations, which biases the $\hat{p}_{ro}(\underline{h})\hat{t}_{ro,ji}(\underline{h})$ cross terms and, in turn, the semivariogram, as discussed more thoroughly by *Ritzi and Allen-King* [2007]. Additional data are currently being collected by taking many more cores with a finer, 0.25 m spacing to characterize lateral lengths at level I, over an extended transect length of 30 m to better characterize the lateral lengths of longer, level II unit types. The goal is to better define the horizontal $\lambda_{\alpha\chi}, \lambda_{\chi\chi}$. These data and results are subject of further research. For now, we can illustrate use of the model by making a few simple assumptions. The composite horizontal integral scale is assumed to be equal to that of *Sudicky* [1986] under the premise that his data, taken over a 20 m transect allowed adequately

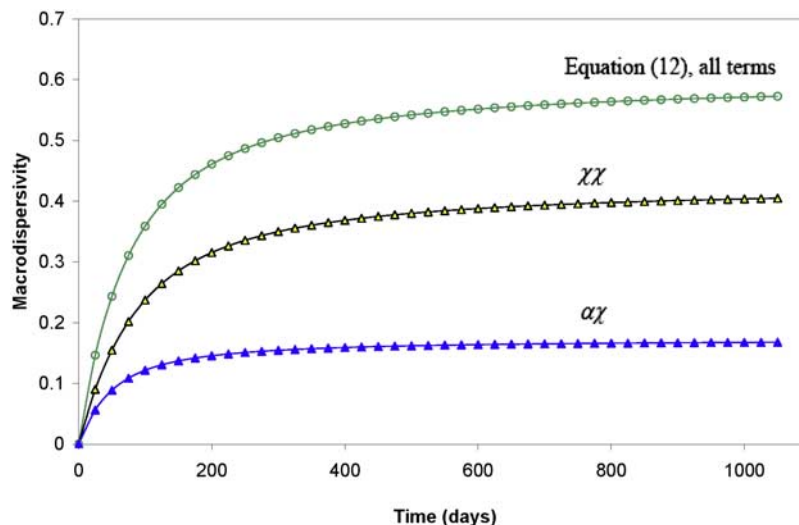


Figure 4. Plot of the longitudinal macrodispersivity.

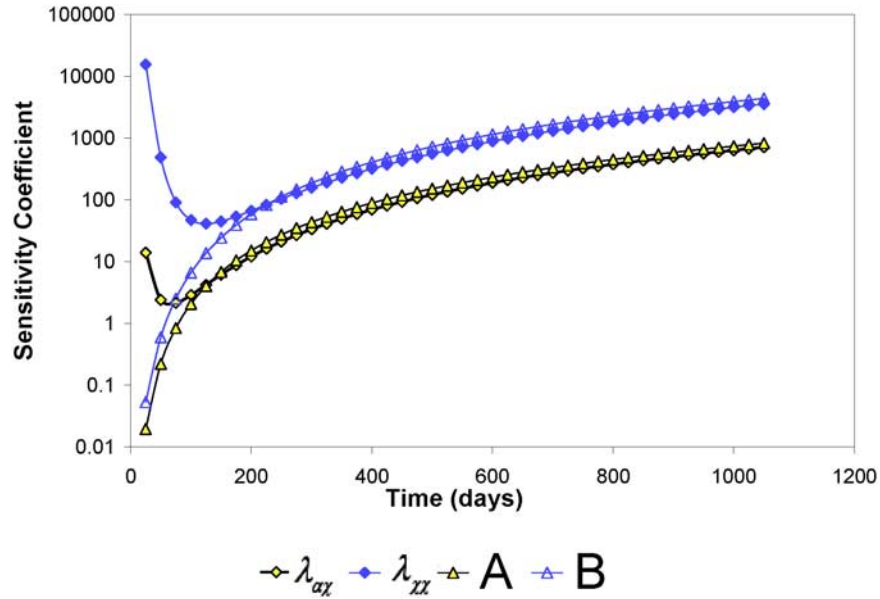


Figure 5. Normalized sensitivity analysis of X_{11} for $\lambda_{\alpha\chi}$, $\lambda_{\chi\chi}$, A , B .

characterizing it (cf. *Ritzi and Allen-King* [2007], whose data were from a transect only 10 m long). Furthermore, a single aspect ratio for the horizontal to vertical correlation scales, ξ , is adopted which is determined as follows.

[23] Let the horizontal integral scales be equal to $\lambda_{\alpha\chi} = \xi a_v$ and, $\lambda_{\chi\chi} = \xi b_v$, where a_v and b_v are the values of the respective vertical integral scales used above. Let σ_s^2 be the exact value of Sudicky's variance (0.29), and λ be the exact value of Sudicky's horizontal integral scale (2.8 m). Therefore, Sudicky's horizontal covariance model is

$$C_Y(h) = \sigma_s^2 e^{-\frac{h}{\lambda}} \quad (18)$$

Let σ_d^2 be the sum of A and B (0.136 and 0.195) from the *Ritzi and Allen-King* [2007] data. A and B are scaled according to σ_s^2/σ_d^2 :

$$A_N = A \times \sigma_s^2/\sigma_d^2; \quad B_N = B \times \sigma_s^2/\sigma_d^2 \quad (19)$$

Substituting these expressions into (9) gives

$$\lambda = \frac{1}{\sigma_s^2} [A_N \xi a_v + B_N \xi b_v] \quad (20)$$

and solving for ξ gives

$$\xi = \frac{\lambda}{\frac{A_N a_v}{\sigma_s^2} + \frac{B_N b_v}{\sigma_s^2}} = 32.7 \quad (21)$$

which is used to compute $[\lambda_{\alpha\chi}, \lambda_{\chi\chi}]$ which, with A_N and B_N , are used to compute equation (16). The result is plotted in Figure 3.

[24] Though the comparisons below are among 2-D models, the 3-D model for the macrodispersion coefficients

can be given if, following *Dai et al.* [2004], we assume an isotropic horizontal integral scale, and account for vertical anisotropy with a transformation of the z coordinate by ξ^{-1} . The corresponding result is

$$\begin{aligned} \frac{D_{11}(t)}{U_1} &= A\lambda_{\alpha\chi} \left\{ 1 - e^{-\tau_{\alpha\chi}} - \xi^{-1} \int_0^\infty \left[(2RJ_1(\beta) \frac{2u^{3/2} - \xi R(2u + \nu)}{\nu^2 u^{3/2}} + F(R)) dR \right] \right. \\ &\quad \left. + B\lambda_{\chi\chi} \left\{ 1 - e^{-\tau_{\chi\chi}} - \xi^{-1} \int_0^\infty \left[(2RJ_1(\beta) \frac{2u^{3/2} - \xi R(2u + \nu)}{\nu^2 u^{3/2}} + F(R)) dR \right] \right\} \right\} \\ F(R) &= \frac{(2 - \beta^2)J_1(\beta) - \beta J_0(\beta)}{R\tau_{\zeta\chi}^2} \frac{\xi^{-3} R^3 (4u + \nu) + (5\nu - 4u)u^{3/2}}{\nu^3 u^{3/2}} \\ \frac{D_{22}(t)}{U_1} &= A\lambda_{\alpha\chi} \xi^{-1} \int_0^\infty \left[\frac{2J_1(\beta) - \beta J_0(\beta)}{\tau_{\alpha\chi}^2} \right. \\ &\quad \left. \bullet \frac{\xi^3 R^3 (4u + \nu) + (5\nu - 4u)u^{3/2}}{R\nu^3 u^{3/2}} \right] dR \\ &\quad + B\lambda_{\chi\chi} \xi^{-1} \int_0^\infty \left[\frac{2J_1(\beta) - \beta J_0(\beta)}{\tau_{\chi\chi}^2} \right. \\ &\quad \left. \bullet \frac{\xi^3 R^3 (4u + \nu) + (5\nu - 4u)u^{3/2}}{R\nu^3 u^{3/2}} \right] dR \\ \frac{D_{33}(t)}{U_1} &= A\lambda_{\alpha\chi} \xi^{-1} \int_0^\infty \left[RJ_1(\beta) \frac{u^{1/2}(4u - 3\nu) - \xi R(4u - \nu)}{\nu^3 u^{3/2}} \right] dR \\ &\quad \cdot B\lambda_{\chi\chi} \xi^{-1} \int_0^\infty \left[RJ_1(\beta) \frac{u^{1/2}(4u - 3\nu) - \xi R(4u - \nu)}{\nu^3 u^{3/2}} \right] dR \end{aligned} \quad (22)$$

where $\beta = R\tau_{\zeta\chi}$, $u = 1 + R^2$, $\nu = 1 + R^2 - \xi^2 R^2$, $\zeta = [\alpha, \chi]$, J_0 and J_1 are the zero and first-order Bessel functions, and R is the variable of integration.

[25] Note that all other assumptions being equal, the 2-D and 3-D models presented in this section reduce to those of *Dai et al.* [2004] if $\lambda_{\alpha\chi} = \lambda_{\chi\chi}$. Furthermore, it is easy to see that the general linear forms of the equations for the hierarchical covariance, macrodispersion coefficients, and particle displacement variance, are all easily expanded for the potential case of additional hierarchical levels that might exist at other sites, by writing the appropriate terms for significant cross-transition groups (e.g., $\alpha\alpha\chi$, $\alpha\chi\chi$, $\chi\chi\chi$, etc.) defined within a hierarchy.

5. Discussion

[26] Figure 3 shows the composite particle displacement variance from equation (16) compared to the corresponding 2-D model from *Sudicky* [1986] and to the observed moments. Though the composite model curve is the same as *Sudicky's* because the same composite integral scale and variance were used, for the purpose of illustration, Figure 3 shows how equation (16) can be used to study the respective contributions from cross-transition structures at each of the two hierarchical levels. Here, there is an indication that the contributions from both $\alpha\chi$ and $\chi\chi$ terms are significant in explaining the particle displacement variance (based on the assumption of a uniform ξ). Furthermore, the contribution of the $\chi\chi$ term is indicated to be greater than the contribution of the $\alpha\chi$ term. Figure 4 illustrates the growth of the macrodispersivity coefficient (equation (12)). Equation (14) gives the asymptotic composite macrodispersivity to be 0.598 m. Furthermore, the contributions of the $\alpha\chi$ and $\chi\chi$ terms to the asymptotic limit are 0.173 m and 0.425 m, respectively and 95% of these contributions are reached after a travel distance of about $28 \lambda_{\alpha\chi}$ and $26 \lambda_{\chi\chi}$, respectively. The normalized sensitivity coefficients are plotted in Figure 5. As centered in the parameter space used above, the model sensitivity to variations in parameters $\{\lambda_{\alpha\chi}, \lambda_{\chi\chi}, A, B\}$ approaches a constant value at about 1050 d. New data collection efforts toward improvements in $\lambda_{\alpha\chi}$ and $\lambda_{\chi\chi}$ seem justified by this result.

6. Conclusions

[27] 1. A centered covariance model in the hierarchical form of equations (8)–(9) represents the hierarchical spatial correlation structure of permeability at the Borden research site, consistent with variography presented by *Ritzi and Allen-King* [2007]. As such, the parameters of the covariance model can be related to quantifiable physical attributes of stratal unit types. The covariance model assumes that $\sum \sum \sigma_{ro}^2 p_{ro}^2$ is small relative to the composite variance, and can be ignored. One reason this assumption is acceptable at Borden is that the σ_{ro}^2 and p_{ro} are each considerably less than unity. *Ritzi et al.* [2004] showed how hierarchical spatial bivariate statistics in this general form can be expanded to represent any number of hierarchical levels, with any number of unit types at each level. Thus, the general approach used here is easily adapted to other sites where this approach is warranted.

[28] 2. The 2-D Lagrangian-based model corresponding to this covariance model is derived as the macrodispersivity tensor coefficients in equations (12)–(13), and as the particle displacement variance in equations (16)–(17). The

3-D version for the macrodispersion coefficients are also given in equation (22). These models link plume spreading to the hierarchical stratal architecture, through the parameters of the hierarchical covariance model. This approach allows for study of the relative contributions, to the composite plume spreading, attributable to permeability differences across smaller-scale level I stratal unit types, and across larger-scale level II stratal unit types, and to the proportions and geometry of these unit types. Thus, the composite dispersion can be linked to quantifiable physical attributes of the stratal architecture.

[29] 3. The macrodispersion models of *Rubin* [1995] and *Dai et al.* [2004] represent one indicator integral scale, but more than one are indicated to be important in relating plume spreading at Borden to hierarchical stratal architecture. The newer model allows cross-transition probabilities at different hierarchical levels to have different integral scales, as indeed shown to be appropriate in representing the hierarchical stratal architecture at the Borden site. This model allows the study of how each scale contributes to the large time limit of the macrodispersivity.

Appendix A: Sensitivity Coefficients of the Particle Displacement Variance X_{11}

[30] Equation (16) is differentiated with respect to integral scales $\lambda_{\alpha\chi}$, $\lambda_{\chi\chi}$, and with respect to A and B .

$$\begin{aligned} \frac{\partial f(\alpha, t)}{\partial \lambda_{\alpha\chi}} = & 2A\lambda_{\alpha\chi} \left[2\tau_{\alpha\chi} - 3 \ln \tau_{\alpha\chi} + \frac{3}{2} - 3E + 3Ei(-\tau_{\alpha\chi}) \right. \\ & \left. + \frac{3(\exp(-\tau_{\alpha\chi}) + \exp(-\tau_{\alpha\chi})\tau_{\alpha\chi} - 1)}{\tau_{\alpha\chi}^2} \right] \\ & + A\lambda_{\alpha\chi}^2 \left[-2\frac{\tau_{\alpha\chi}}{\lambda_{\alpha\chi}} + \frac{3}{\lambda_{\alpha\chi}} + \frac{3\exp(-\tau_{\alpha\chi})}{\tau_{\alpha\chi}} \right. \\ & \cdot \left(\frac{1}{\lambda_{\alpha\chi}} + \frac{\exp(-\tau_{\alpha\chi})}{ut} \right) + 3 \left(\frac{\exp(-\tau_{\alpha\chi})}{ut} \left(1 + \frac{2}{\tau_{\alpha\chi}} \right) \right. \\ & \left. \left. + \frac{\exp(-\tau_{\alpha\chi})}{ut} (\tau_{\alpha\chi} + 1) - \frac{2}{\tau_{\alpha\chi}} \frac{1}{ut} \right) \right] \quad (A1) \end{aligned}$$

$$\begin{aligned} \frac{\partial f(\alpha, t)}{\partial \lambda_{\chi\chi}} = & 2B\lambda_{\chi\chi} \left[2\tau_{\chi\chi} - 3 \ln \tau_{\chi\chi} + \frac{3}{2} - 3E + 3Ei(-\tau_{\chi\chi}) \right. \\ & \left. + \frac{3(\exp(-\tau_{\chi\chi}) + \exp(-\tau_{\chi\chi})\tau_{\chi\chi} - 1)}{\tau_{\chi\chi}^2} \right] \\ & + B\lambda_{\chi\chi}^2 \left[-2\frac{\tau_{\chi\chi}}{\lambda_{\chi\chi}} + \frac{3}{\lambda_{\chi\chi}} + \frac{3\exp(-\tau_{\chi\chi})}{\tau_{\chi\chi}} \right. \\ & \cdot \left(\frac{1}{\lambda_{\chi\chi}} + \frac{\exp(-\tau_{\chi\chi})}{ut} \right) + 3 \left(\frac{\exp(-\tau_{\chi\chi})}{ut} \left(1 + \frac{2}{\tau_{\chi\chi}} \right) \right. \\ & \left. \left. + \frac{\exp(-\tau_{\chi\chi})}{ut} (\tau_{\chi\chi} + 1) - \frac{2}{\tau_{\chi\chi}} \frac{1}{ut} \right) \right] \quad (A2) \end{aligned}$$

$$\begin{aligned} \frac{\partial f(\alpha, t)}{\partial A} = & \lambda_{\alpha\chi}^2 \left[2\tau_{\alpha\chi} - 3 \ln \tau_{\alpha\chi} + \frac{3}{2} - 3E + 3Ei(-\tau_{\alpha\chi}) \right. \\ & \left. + \left(\frac{3(\exp(-\tau_{\alpha\chi}) + \exp(-\tau_{\alpha\chi})\tau_{\alpha\chi} - 1)}{\tau_{\alpha\chi}^2} \right) \right] \quad (A3) \end{aligned}$$

$$\frac{\partial f(\alpha, t)}{\partial B} = \lambda_{xx}^2 \left[2\tau_{xx} - 3 \ln \tau_{xx} + \frac{3}{2} - 3E + 3Ei(-\tau_{xx}) + \left(\frac{3(\exp(-\tau_{xx}) + \exp(-\tau_{xx})\tau_{xx} - 1)}{\tau_{xx}^2} \right) \right] \quad (\text{A4})$$

[31] **Acknowledgments.** This work was supported by the National Science Foundation under grants EAR-0510819 and EAR-0538037. Any opinions, findings, and conclusions or recommendations expressed in this paper are those of the authors and do not necessarily reflect those of the National Science Foundation.

References

- Barrash, W., and T. Cleo (2002), Hierarchical geostatistics and multifacies systems: Boise Hydrogeophysical Research Site, Boise, Idaho, *Water Resour. Res.*, 38(10), 1196, doi:10.1029/2002WR001436.
- Benjamin, J. R., and A. C. Cornell (1970), *Probability, Statistic, and Decision for Civil Engineers*, 684 pp., McGraw-Hill, New York.
- Dagan, G. (1982), Stochastic modeling of groundwater flow by unconditional and conditional probabilities: 2. The solute transport, *Water Resour. Res.*, 18(4), 835–848, doi:10.1029/WR018i004p00835.
- Dagan, G. (1984), Solute transport in heterogeneous porous media, *J. Fluid Mech.*, 145, 151–177, doi:10.1017/S0022112084002858.
- Dagan, G. (1989), *Flow and Transport in Porous Formations*, 465 pp., Springer, New York.
- Dai, Z., R. W. Ritzi, C. C. Huang, D. F. Dominic, and Y. N. Rubin (2004), Transport in heterogeneous sediments with multimodal conductivity and hierarchical organization across scales, *J. Hydrol.*, 294(1–3), 68–86, doi:10.1016/j.jhydrol.2003.10.024.
- Dai, Z., R. W. Ritzi, and D. F. Dominic (2005), Improving permeability semivariograms with transition probability models of hierarchical sedimentary architecture derived from outcrop analog studies, *Water Resour. Res.*, 41, W07032, doi:10.1029/2004WR003515.
- Freyberg, D. L. (1986), A natural gradient experiment on solute transport in a sand aquifer: 2. Spatial moments and the advection and dispersion of nonreactive tracers, *Water Resour. Res.*, 22(13), 2031–2046.
- Lu, Z., and D. Zhang (2002), On stochastic modeling of flow in multimodal heterogeneous formations, *Water Resour. Res.*, 38(10), 1190, doi:10.1029/2001WR001026.
- Neuman, S. P. (2003), Relationship between juxtaposed, overlapping, and fractal representations of multimodal spatial variability, *Water Resour. Res.*, 39(8), 1205, doi:10.1029/2002WR001755.
- Neuman, S. P. (2006), Comment on “Spatial correlation of permeability in cross-stratified sediment with hierarchical architecture” by Robert W. Ritzi, Zhenxue Dai, David F. Dominic, and Yoram N. Rubin, *Water Resour. Res.*, 42, W05601, doi:10.1029/2005WR004256.
- Proce, C. J., R. W. Ritzi, D. F. Dominic, and Z. Dai (2004), Modeling multiscale heterogeneity and aquifer interconnectivity, *Ground Water*, 42(5), 658–670, doi:10.1111/j.1745-6584.2004.tb02720.x.
- Rajaram, H., and L. W. Gelhar (1991), Three-dimensional spatial moments analysis of the Borden tracer test, *Water Resour. Res.*, 27(6), 1239–1251.
- Ritzi, R. W. (2000), Behavior of indicator variograms and transition probabilities in relation to the variance in lengths of hydrofacies, *Water Resour. Res.*, 36(11), 3375–3381, doi:10.1029/2000WR900139.
- Ritzi, R. W., Jr., and R. M. Allen-King (2007), Why did Sudicky [1986] find an exponential-like spatial correlation structure for hydraulic conductivity at the Borden research site?, *Water Resour. Res.*, 43, W01406, doi:10.1029/2006WR004935.
- Ritzi, R. W., Z. Dai, D. F. Dominic, and Y. N. Rubin (2004), Spatial correlation of permeability in cross-stratified sediment with hierarchical architecture, *Water Resour. Res.*, 40(3), W03513, doi:10.1029/2003WR002420.
- Ritzi, R. W., Z. Dai, D. F. Dominic, and Y. N. Rubin (2006), Reply to comment by Shlomo P. Neuman on “Spatial correlation of permeability in cross-stratified sediment with hierarchical architecture” by Robert W. Ritzi, Zhenxue Dai, David F. Dominic, and Yoram N. Rubin, *Water Resour. Res.*, 42, W05602, doi:10.1029/2005WR004402.
- Rubin, Y. (1995), Flow and transport in bimodal heterogeneous formations, *Water Resour. Res.*, 31(10), 2461–2468, doi:10.1029/95WR01953.
- Rubin, Y. (2003), *Applied Stochastic Hydrogeology*, Oxford Univ. Press, Oxford, U. K.
- Rubin, Y., I. A. Lunt, and J. S. Bridge (2006), Spatial variability in river sediments and its link with river channel geometry, *Water Resour. Res.*, 42, W06D16, doi:10.1029/2005WR004853.
- Sudicky, E. A. (1986), A natural gradient experiment on solute transport in a sand aquifer: Spatial variability of hydraulic conductivity and its role in the dispersion process, *Water Resour. Res.*, 22(13), 2069–2082, doi:10.1029/WR022i013p02069.
- Weissmann, G. S., and G. E. Fogg (1999), Multi-scale alluvial fan heterogeneity modeled with transition probability geostatistics in a sequence stratigraphic framework, *J. Hydrol.*, 226(1–2), 48–65, doi:10.1016/S0022-1694(99)00160-2.
- Weissmann, G. S., S. F. Carle, and G. E. Fogg (1999), Three dimensional hydrofacies modeling based on soil surveys and transition probability geostatistics, *Water Resour. Res.*, 35(6), 1761–1770, doi:10.1029/1999WR900048.
- Woodbury, A. D., and E. A. Sudicky (1991), The geostatistical characteristics of the Borden aquifer, *Water Resour. Res.*, 24(7), 533–546, doi:10.1029/90WR02545.

C. Huang, Department of Mathematics and Statistics, Wright State University, Dayton, OH 45430, USA.

R. Ramanathan and R. W. Ritzi, Jr., Department of Earth and Environmental Sciences, Wright State University, Dayton, OH 45430, USA. (robert.ritzi@wright.edu)